This manuscript has been published in the Engineering Structures 2018, Vol. 166, pp. 79-92.
doi.org/10.1016/j.engstruct.2018.03.062

Direct Design Method for space frames with cold–formed steel hollow sections

Wenyu Liu, Hao Zhang*, Kim Rasmussen
The University of Sydney

Keywords: Cold-formed steel; Advanced Analysis with Imperfections; nonlinear frame analysis; structural reliability; system-based design; building standards (codes).

Abstract

Design-by-analysis methods for steel structures are receiving considerable attention from professional engineers, researchers and standard-writing groups. Designing by analysis, termed as the Direct Design Method (DDM), is premised on the use of geometric nonlinear inelastic finite element analysis to determine the ultimate strength of steel structural frames and subsequently incorporating a *system* resistance factor (ϕ_s) to account for the effects of uncertainties in geometric parameters, stiffness and strength. This paper outlines the DDM in the context of cold-formed compact Hollow Steel Sections (HSS), including the reliability analysis framework at system level underpinning the Method. The system resistance factors for a series of representative 3D frames with hollow locally stable cross-sections are derived.

1. Introduction

Steel structures are traditionally designed by a combination of a frame analysis that provides the internal actions and a design specification which provides rules for calculating the strength of members and connections for the set of internal actions (forces and moments) determined from the structural analysis. While in the past 40 years the structural frame analysis has shifted from hand-calculated based analysis to second-order elastic analysis, the two-step design approach has been utilised extensively for more than one hundred years. With the advances in structural engineering during the past two decades, the behaviour of a highly redundant structural steel system can now be precisely determined by nonlinear finite element analysis, which may be a beam element-based plastic zone analysis for compact sections, or shell element-based large deformation inelastic analysis for structures with thin-walled members prone to distortional as well as local instabilities [1-7]. The advanced nonlinear finite element analysis provides engineers an opportunity to move from the two step member-based design method to a system-based approach.

This manuscript has been published in the Engineering Structures 2018, Vol. 166, pp. 79-92. *Corresponding author
doi.org/10.1016/j.engstruct.2018.03.062

In this paper, the direct design by analysis approach is referred to as "Direct Design Method" (DDM). The DDM provides the unique feature such that system failure (ultimate frame strength) rather than member limit state is regarded as the design criterion. The frame analysis in the DDM shall incorporate all sources of important nonlinear actions affecting the structural behaviour, notably second-order effects, plasticity, semi-rigidity of connections, residual stress, initial geometric imperfection, and be able to detect all the relevant limit states (e.g., sectional yielding and member buckling) covered by the specification equations. The essence of the DDM is that the structure is modelled as realistically as possible, to the point of accurately simulating the structural response that one would achieve in physical tests of the structure. Such an analysis is termed "advanced analysis" in AS4100 [8], "inelastic method" in AISC360-10 [9], and "geometrical and material nonlinear analysis with imperfections" in European terminology. Modern FE analysis software such as ANSYS, Strand 7, ABAQUS, and the open-source OpenSEES software increasingly feature material and geometric nonlinear analyses which may employ beam elements and/or shell elements. Technically, the application of advanced structural analysis for system-based design has diminished considerably, especially seeing that the performance of standard desktop computers now allows sizeable structures to be analysed by advanced analysis sufficiently quickly to be a practical proposition.

The DDM has significant practical advantages over the conventional member-based design methods. By using the advanced analysis, the failures of member and connection can be explicitly assessed within a structural frame system and subsequently, the capacities of the member and connection can be directly checked without the use of design strength provisions of a structural standard. Apart from generally leading to lighter frames, the DDM provides a conceptually simple method of design with more uniform reliability of a wide spectrum of steel frames [10]. It also informs the designer of the failure mode and the complete path from elastic to ultimate and post-ultimate, enabling the designer to consider the consequences of failure, thus providing further incentive for using the Method.

The approach for design based on advanced analysis of the overall structural frame behaviour have been incorporated into several steel design standards(e.g., [8, 9]) (except for earthquake design). However, even with sophisticated nonlinear finite element analysis, the true behaviour of a steel structure cannot be evaluated with certainty because numerous sources of uncertainty exist in structural loads, strength and stiffness of system, members and connections. These

uncertainties give rise to risk and introduce a probability of failure. In *load and resistance factor design* (LRFD), member reliability requirements are achieved through the resistance factors using a reliability calibration process [11, 12]. However, the system-based DDM has yet to address the problem of satisfying the minimum system-based reliability requirement.

This paper outlines the DDM and the reliability analysis framework at system level underpinning the Method. The procedures of probabilistically deriving the system resistance factor for the DDM are presented with particular emphasis on 3D cold-formed steel frames with compact hollow sections. Sixteen baseline frames (eight moment frames and eight braced frames) with different configurations and failure modes are investigated. The system resistance factors corresponding to different levels of target reliability are derived.

2. DIRECT DESIGN METHOD

In the DDM, the frame analysis and design check are achieved in one integrated step, taking the LRFD format,

$$\phi_s R_n \geq \sum \gamma_i Q_{ni} \tag{1}$$

where R_n is the nominal ultimate strength of the frame predicted by advanced analysis using the nominal geometric and material properties while ϕ_s is a system resistance factor that considers the effects of uncertainties in frame strength, geometric properties and stiffness, Q_{ni} are applied nominal loads (gravity, wind loads) to the whole frame, and γ_i are load factors from the loading standards (e.g., ASCE7-05 [13]).

When conducting a nonlinear finite element analysis, the frames' ultimate strength is predicted using a static pushdown analysis for gravity loads, or a static pushover analysis for combined wind and gravity loads. The loads are increased proportionally and incrementally in the analysis until system failure. The peak point of the load-displacement response is determined as the frames' ultimate strength. In case of there is no descending branch in the load-deflection response, the frame's ultimate strength is chosen as the point where the gradient of the load-displacement response is decreased to 5% of its initial gradient [14]. The applied load is often expressed as the product of a scaling load factor λ and a reference applied load. Thus, Eq. (1) is equivalent to $\lambda_u \geq 1/\phi_s$, in which $\lambda_u$is denoted as the ultimate frame load factor.

3. SYSTEM RELIABILITY ASSESSMENT

The system resistance factor ϕ_s in Eq. (1) needs to be determined using concepts of probabilistic limit state design accounting for the uncertainties in loads and system resistance to achieve a design with the predefined level of system reliability [12]. In the structural reliability theory, the safety of a structure is quantified by its probability of failure, P_f, i.e., the likelihood of reaching the limit state(s) during its lifetime. Monte Carlo Simulation (MCS) is regarded as a conventional approach for determining the probability of failure of a structure. This technique involves (1) in each simulation, randomly generating values of the uncertain properties within a structural (e.g., elastic modulus, yield stress, residual stress, initial geometric imperfections, strain hardening etc.) and the loads according to their statistical characteristics, and (2) checking if the ultimate strength of the frame predicted using advanced analysis is equal to or greater than the total applied loads. After a sufficient number of simulations, the probability of failure can be numerically estimated as $P_f = n/N$, in which N is denoted as the total number of simulations performed, and n represents the number of simulations where the structure cannot withstand the applied loads. More advanced simulation-based methods using variance-reduction techniques are also available for system reliability evaluations [15-18]. In probability-based structural design, the so-called reliability index, β, is customarily used as an alternative of reliability to P_f, with the relationship $\beta = \Phi^{-1}(1-P_f)$, where Φ^{-1} is denoted as the inverse of the distribution function of a standard normal distribution [12, 19].

For a cold-formed steel structure, the important random variables that need to be accounted for in reliability analyses include: structural loads, yield stress, Young's modulus, residual stress, cross-sectional properties, and initial geometric imperfections. Furthermore, the inherent randomness in material properties and loads, the model uncertainty of advanced analysis also needs to be considered. The probabilistic characteristics for these uncertainties will be discussed in detail in Section 4.

The computational cost of the aforementioned direct Monte Carlo method can be very intensive, because each simulation requires a nonlinear structural analysis. The direct Monte Carlo method is impractical for code-development which involves system reliability evaluations of a large number of steel frames. To overcome this difficulty, the First-Order Reliability Method (FORM) [19, 20] is adopted for system reliability assessment in this study. In this approach, the stochastic characteristics of a steel frame are first estimated using a relatively small number of simulations, and subsequently combined with the statistics of applied structural loads to estimate the

131 probability of failure.
132
133 Consider a steel frame at its limit under the gravity load combination 1.2 D_n+1.6 L_n specified in
134 ASCE7-05 [13], in which D_n and L_n are the nominal dead and live loads, respectively. The design
135 equation of Eq. (1) becomes

$$\phi_s R_n = 1.2D_n + 1.6L_n. \quad (2)$$

136 The associated limit state function g is
137

$$g = R_G - D - L \quad (3)$$

138 in which R_G is denoted as the frames' resistance to gravity loads, D = dead load, and L represents
139 the (maximum lifetime) live load. The frame fails if the limit state function g is less than zero.
140
141 For a frame under both wind and gravity loads, the design load combination is
142

$$\phi_s R_n = 1.2D_n + 0.5L_n + 1.6W_n \quad (4)$$

143 where W_n is the nominal wind load from ASCE7-05. Note that Eq. (4) represents the load
144 combination of dead load, wind load, and the "arbitrary point-in-time" live load. Accordingly,
145 the limit state function can be expressed as:
146

$$g = R_w - W \quad (5)$$

147 where R_w is the system lateral capacity when the frame is subjected to the applied dead load and
148 the "arbitrary point-in-time" live loads, and W represents the wind load.
149
150 The probabilistic models for structural loads (dead load, life-time maximum live load, arbitrary
151 point-in-time live load and life-time maximum wind loads) are available from previous research
152 [21]. The resistance models of R_G and R_w can be estimated using the MCS, considering the
153 uncertainties in geometric and material properties as well as the model uncertainty of the
154 advanced analysis. The efficiency of MCS technique may be enhanced by Latin Hypercube
155 Sampling (LHS). Typically, 350 to 550 simulations based on LHS are sufficient for estimating
156 the probabilistic characteristics (mean, variance, distribution type) of system resistance. Provided

157 the statistics of the structural loads and system resistance are available, the structural reliability
158 can be promptly evaluated by applying the FORM [22, 23].
159
160 Using the aforementioned system reliability analysis method, the β-ϕ_s curve for a frame can be
161 obtained.This curve provides a basis for choosing the system resistance factor for any target
162 system reliability requirement.
163
164 When developing the design criteria for the DDM, a critical issue is how to define the baseline
165 systems to be analysed as there are numerous systems in the real world. The purpose of the study
166 is not to analyse as many systems as possible; rather, one needs to search the common
167 characteristics of system reliabilities which allow the results of these analyses to be generalized,
168 e.g., frame layout (regular or irregular, braced or unbraced) and failure mode.
169
170 **4. UNCERTAINTIES IN COLD-FORMED HSS FRAME SYSTEMS**
171 For cold-formed HSS frames, the important random variables that need to be addressed in
172 reliability analyses include: elastic modulus, yield stress, structural loads residual stress, cross-
173 section properties, and initial geometric imperfections. Moreover, using nonlinear finite element
174 analysis introduces *model uncertainty*. All the important uncertainties, including model
175 uncertainty must be addressed in the DDM design process.
176
177 Table 1 presents the statistics for some of the random variables that are readily obtained from
178 the literature, including the yield stress (F_y), elastic modulus (E), cross-section thickness (t) of
179 HSS, and the loads. Note that the "L" in Table 1 represents the maximum live load in 50 years,
180 while L_{apt} represents the arbitrary point-in-time live load. The probabilistic models of other
181 uncertain parameters are discussed in this section.
182 **4.1. Uncertainty in initial geometric imperfections**
183
184 The method proposed in [24] is used for modelling the initial geometric imperfections. In this
185 method, the superposition of a certain number of buckling modes of a column in compression is
186 utilized to represent the member initial out-of-straightness:

$$\delta = \gamma \sum_{i=1}^{m} a_i \sin(i\pi x) \tag{6}$$

187 in which $x \in [0,1]$ represents the normalized coordinate along the member length, a_i is the scale
188 factor for the ith buckling mode, which is random, δ denotes the out-of-straightness at x and γ is

189 a random sign indicator (either +1 or −1) to denote the direction of imperfection. Previous study
190 has indicated that the member out-of-straightness can be sufficiently modelled using the first
191 three modes [25].
192
193 Three sets of data which comprise of one from Milan Polytechnic University [26] and two from
194 the University of Sydney [27] were used to derive the scale factor a_i in Eq. (6) for HSS. The
195 statistics of each of the scale factors are summarised in Table 2, modelled with a lognormal
196 distribution. In a 3D analysis, the member imperfections of a member are treated as random
197 variables for both cross-sectional axes with no correlation.
198
199 The out-of-plumbness of frame is also modelled as a random variable. It is assumed that all
200 columns lean in one direction with respect to each cross-sectional axis. This is a conservative
201 assumption. The statistical data for frame out-of-plumbness have been reported in [25]. The out-
202 of-plumbness angle is descripted by a lognormal, whose mean value is 1/770 and standard
203 deviation is 1/880.
204
205 **4.2. Uncertainty in residual stress**
206 The residual stress in non-stress-relieved cold-formed steel sections has various components (i.e.,
207 membrane, bending and layering residual stresses in the longitudinal and transversal directions).
208 The effects of different components of the residual stress on the ultimate strength of a cold-
209 formed steel frame has been investigated in the literature, e.g., [29]. In general, the bending
210 residual stress in the longitudinal direction has a more dominant influence on the system's
211 ultimate strength than other components of the residual stress. Thus, the effect of residual stress
212 in cold-formed HSS can be reasonably considered by only modelling the longitudinal bending
213 residual stress [29].
214
215 Following the approach in [29], the present study modified the steel's stress-strain curve to
216 simulate the effect of residual stress. The detail of this method can be found in [28, 29]. Equations
217 (7-9) give the modified stress-strain curve for cold-formed HSS which takes into account the
218 effect of longitudinal bending residual,
219

$$\sigma = E\varepsilon \quad \text{for} \quad 0 < \varepsilon < \varepsilon_1 \tag{7}$$

$$\sigma = \frac{2F_y - E\varepsilon_1 - E\varepsilon_2}{(\varepsilon_1 - \varepsilon_2)^3}\varepsilon^3 + \frac{2\varepsilon_1^2 E + 2\varepsilon_1\varepsilon_2 E + 2\varepsilon_2^2 E - 3\varepsilon_1 F_y - 3\varepsilon_2 F_y}{(\varepsilon_1 - \varepsilon_2)^3}\varepsilon^2 + \frac{4\varepsilon_1^2\varepsilon_2 E + \varepsilon_1\varepsilon_2^2 E + \varepsilon_2^3 E - 6\varepsilon_1\varepsilon_2 F_y}{(\varepsilon_2 - \varepsilon_1)^3}\varepsilon + \frac{2\varepsilon_1^2\varepsilon_2^2 E + \varepsilon_1^3 F_y - 3\varepsilon_1^2\varepsilon_2 F_y}{(\varepsilon_1 - \varepsilon_2)^3} \quad \text{for } \varepsilon_1 < \varepsilon < \varepsilon_2 \tag{8}$$

$$\sigma = F_y \quad \text{for} \quad \varepsilon > \varepsilon_2 \tag{9}$$

where the non-linear transition from the elastic to yield are defined by the two parameters ε_1 and ε_2, which can be solved by Eq. (10) and Eq. (11), respectively:

$$\varepsilon_1 = \frac{F_y}{E} - \frac{\sigma_b}{E}, \tag{10}$$

and

$$\varepsilon_2 = \frac{\sigma_b}{E} + \frac{F_y}{E}, \tag{11}$$

where σ_b is denoted as the actual magnitude of bending surface residual stress in the longitudinal direction. Figure 1 schematically compares the elastic-plastic material model and the modified stress-strain model according to Eqs. (7-9). Details about the model can be found elsewhere [29].

The uncertainty of the residual stress of HSS is considered by modelling the longitudinal bending residual stress (σ_b) as a random variable. The statistics of σ_b is summarised based on the experimental surface residual stress measurements of 35 experimental samples. Based on this result, the coefficient of variation (COV) for σ_b is 0.05 while the mean is found to have a value of $0.7F_y$ [29].

4.3. Model uncertainty

In addition to the inherent random variations in material and geometric properties and structural loads, the model uncertainty of nonlinear finite element analysis also needs to be considered. Model uncertainty arises from assumptions and approximations made in finite element modelling and analysis, such as the use of two-dimensional models to represent three-dimensional structures, simplified boundary conditions and idealized connection behaviour, neglecting non-structural elements, and introducing discretisation errors in the finite element modelling, etc. In theory, the model uncertainty of advanced analysis might be estimated by comparing

experimental results of frame load tests to the predicted results from advanced analysis. However, only limited full-scale load test results are available in the literature, e.g., for cold-formed steel portal frames [30] and steel rack structures [31]. Based on these frame tests, the model uncertainty of the advanced analysis for portal frames was estimated as having a bias factor of 0.92 and a COV of 0.061. For rack structures, the model uncertainty has a mean of 1.13 and a COV = 0.065. For three-dimensional cold-formed HSS frames (with compact sections) considered in this study, no frame tests are available to estimate the model uncertainty. It is assumed that with current plastic-zone type nonlinear finite element software, the model uncertainty for 3D hollow structural section frames without local buckling is unbiased and its COV is relatively small, assumed to be 0.05.

5. SYSTEM RESISTANCE FACTORS FOR THREE-DIMENSIONAL COLD-FORMED HSS FRAMES

A set of eight 3D HSS moment frames and eight HSS braced frames were selected in the present study as the baseline structures to derive ϕ_s for the DDM. The layouts for the moment frames and braced frames are demonstrated in Figs 2 and 3, respectively. The details about the member sizes of the sixteen frames can be found elsewhere [28].All members are fully compact cold-formed square hollow sections, i.e. local instability is not considered in the study.

5.1. Advanced analysis models

The six degree-of-freedom three-dimensional beam element (B31) in ABAQUS is used for the frame analysis, which considers beam shear deformation but neglects warping torsion. Both in-plane and out-of-plane behaviours are considered in the frame analysis.

Beam-column joints are assumed rigid for the moment-resisting frames and with sufficient ductility to preclude fracture. Thus, compliance of the connections is not considered in this study. For the braced frames, the beam-column joints are hinged. A simple X-bracing system is utilized in the braced frame as the statistical characteristics of the frame ultimate strength is found insensitive to the layout of the bracing system. The failure of brace members is precluded.

The steel stress-strain curve is described using the material model in Eqs. (7-9) to capture the effect of residual stress. The steel has an elastic modulus of 200 GPa and a nominal value of yield stress F_{yn} of 450 MPa. The nominal value for the longitudinal bending residual stress (σ_b) is equal to $0.7F_{yn}$ (315 MPa).

The nominal frame out-of-plumbness has a nominal value of $H/770$ and was modelled by the Notional Horizontal Load method. This value is based on the mean value of the out-of-plumbness, as described in Section 4.1. The out-of-straightness of the component HSS members was not modelled in the nominal frame models, consistent with current engineering practice. However, the member out-of-straightness was included in the Monte Carlo simulations.

The uniformly distributed floor pressures on slabs are converted to line loads applied along the beams based on the tributary areas. The wind loads are converted to concentrated loads applied on the beam-to-column connections. Rigid diaphragms are introduced at each storey level to simulate the effect of floor slabs. To model the rigid diaphragm in the beam-element based frame model, the planar translation and twist rotation degrees-of-freedom of the nodes along the beams at each floor is kinematically constrained. Consequently, the existence of a rigid diaphragm allows in-plane bending of the beams in the vertical direction while it provides lateral and torsional restraint to out-of-plane bending. Details about the modelling of rigid diaphragms can be found in [32].

As a structure's reliability may be dependent on its mode of failure, a variety of failure modes need to be considered. For each baseline frame, the member sizes were adjusted to induce different failure modes such as frame sway instability and formation of plastic hinges. Thus, each baseline frame is expanded into several related frames, with the same frame configurations and loads, but different member sizes [2, 22, 28].

In this study, a plastic-zone type of analysis is employed to model the development of plasticity along the member and through the cross-sections. The criterion for forming a "plastic hinge" is therefore based on the cross-sectional yield ratio exceeding a certain threshold. To determine this threshold, a simply supported beam of 8 m was considered. The cross-section of the beam is a square hollow section (250×250×16 mm), with a nominal Young's modulus of 200 GPa and a nominal yield stress of 450MPa. A point load is applied vertically at the mid-span. The beam was analysed using a plastic hinge analysis and a plastic zone analysis, respectively. It was found that when a plastic hinge has formed in the plastic hinge analysis, the corresponding cross-sectional yield ratio given by the plastic zone analysis is 62.5%. Therefore, in this study, if 62.5% of a cross-sectional area has yielded, it represents the case of significant yielding and can be considered as a plastic hinge. If a yield ratio of 62.5% or more is found within the cross-section

of any beam or column, the failure mode is defined as Fully Yielded (FY). Otherwise the failure mode is referred to as Partially Yielded (PY).

5.2. Moment-resisting HSS frames under gravity loads

In this section, the sample distribution of the 16 baseline frames' gravity resistance were generated by performing MCS using LHS technique. 300 random samples of each baseline frame were simulated with random values for the yield stress, Young's modulus, cross-section thickness, longitudinal residual stress, member out-of-straightness, and frame out-of-plumbness according to their statistics presented in Section 4. Perfect correlation is assumed for the random properties (F_y, E and t) between all members. Studies have shown that the perfect correlation assumption is usually conservative for reliability evaluations [34].

Through the Monte Carlo simulation, the mean-to-nominal ratios and COV's of the eight baseline moment frames' gravity resistance were obtained and presented in Table 3. It was found that the strength statistics of all these frames are comparable despite their different modes of failure (BFY-CFY, BFY-CPY, etc.) and configurations (regular and irregular).The mean-to-nominal values for the strengths vary from 0.99 to 1.08, with the COV varying from 0.09 to 0.123. The average mean-to-nominal ratio and COV for the strengths of these baseline frames are 1.04 and 0.11, respectively. A lognormal distribution can reasonably fit the Monte Carlo samples of the frames' gravity resistance. The simulated sample distribution of Frame 3 with a failure mode of BFY-CFY is plotted in Fig. 4(a) as an example. The full set of resistance distributions for all baseline frames are given in [25].

Since live load has more variability than dead load, a structure's reliability is dependent on the live-to-dead load ratio. Typical nominal load ratios L_n/D_n for light gauge cold-formed steel structures vary from 1.0 to 5.0 [33]. Clearly, one cannot achieve a uniform reliability for different L_n/D_n ratios by using a single value of ϕ_s. However, for daily engineering practice, a constant resistance factor for all loading scenarios has its practical advantages. To calculate the "average" value of ϕ_s, each case of L_n/D_n is assigned a relative weight as shown in Table 4 [33]. The weights represent the relative frequency of occurrence of different L_n/D_n ratios.

With the system resistance models obtained from the Monte Carlo simulations and the stochastic load models obtained from the literature, the system resistance factors of the frames were

computed for four levels of target reliability index (β= 2.5, 2.75, 3.0 and 3.5) using the FORM outlined in previous sections. Table 3 summarizes the results. It can be seen that ϕ_s for the eight baseline moment frames are similar although the frame configuration and failure modes are different. Note that the resistance factors are the "weighted-average" values of different cases of live-to-dead load (L_n/D_n) ratios given in Table 4. As a demonstration, Fig. 4(b) shows the β-ϕ_s relationship for Frame 3 with a failure mode of BFY-CFY. As expected, β decreases with increasing ϕ_s. For a given value of ϕ_s, β decreases as L_n/D_n increases.

The target reliability index for hot-rolled steel members in the current LRFD of steel structures is approximately 2.6-2.8 under gravity loads [32, 34]. The target member reliability index for cold-formed steel members designed by the American Standard AISI-S100 or Australian Standard AS4600 the is about 2.5 under gravity loads. If the target system reliability index for the DDM is assumed to be comparable to the member reliability, i.e., fall in the range 2.5 to 3.0 under gravity loads, Table 3 shows that the weighted-average value of ϕ_s needs to be 0.87 if the target reliability index is 2.5, and changes to 0.77 for a target reliability index of 3.

5.3. HSS moment frames subjected to combined wind and gravity loads

Next, the HSS moment frames under both wind and gravity loads is considered. ASCE7-05 describes four wind load cases: Case 1, applying full wind load and considered separately for each direction; Case 2: applying three quarters of the wind load in conjunction with a torsional moment, considered separately for each direction; Case 3: applying three quarters of the wind load, considered to act simultaneously in both directions; and Case 4: analogy to Case 2, but applying the wind loads at 75% of the specified value. For each baseline frame, the most critical wind load case was determined, and subsequently used in the reliability assessments to determine the resistance factors.

For the eight basis moment frames, the probabilistic models for their lateral resistance were obtained through Monte Carlo simulation. In each simulation, a dead load and an arbitrary point-in-time live load are sampled from their distributions and applied to randomly generated frame. The gravity loads are applied first, and subsequently the ultimate lateral resistance of the frame can be obtained from a static pushover analysis which increasing the lateral load until the frame collapse. As detailed in [25], the uncertainties in R_w for the eight baseline moment frames are comparable, with a COV varying between 0.10 and0.16. A lognormal distribution can reasonably

fit R_w. The distribution of R_w for Frame 3 subjected to wind load Case 1 is shown in Fig. 5, including a fitted lognormal distribution.

In the reliability analyses, the dead-to-live load ratio is fixed as L_n/D_n= 2.0, considered to be a typical live to dead load ratio for HSS structures. Three typical values of wind-to-gravity load ratios ($W_n/(L_n+D_n)$) are considered, i.e., $W_n/(L_n+D_n)$ = 0.05, 0.1, and 0.15, with the relative weights of 30%, 40%, and 30%, respectively.

The weighted-average values of ϕ_s for the eight baseline moment frames are presented in Table 5 for four levels of target reliability index. As an example, Fig. 6 plots the β-ϕ_s curves for moment Frame 3. From Table 5, it can be observed that the ϕ_s varies from 0.71 to 0.75, with an average value of 0.73 when β of 2.75 is considered, and this value of ϕ_s is increased to 0.81 when a value of β of 2.5 is considered. A comparison of Tables 3 and 5 demonstrates that the ϕ_s–values for wind loading are lower than the ϕ_s–values for gravity loads only. This is not surprising because the wind load is more uncertain than gravity loads. Based on Tables 3 and 5, it can be found that using a system resistance factor of 0.85 would lead to a system reliability index of about 2.7 for gravity loads only, and 2.4 for wind loads.

From the study it was also found that the ϕ_s are not affected by the presence of rigid diaphragms representing floor slabs, or wind load cases (uni-directional or bi-directional) [25].

5.4. HSS braced frames subjected to gravity loads only

The system resistance factors for the eight HSS hinge joint braced frames are summarized in Table6. Resistance distributions and β-ϕ_s curves for Braced Frame 3are shown in Fig. 7. It is observed that the system resistance factors summarised in Table 6 are comparable to the results for moment frames presented in Table 3, suggesting that the same resistance factors can be used for both moment frames and braced frames.

5.5. Serviceability reliabilities of moment HSS frames

As compared to elastic design, the serviceability performance may become more important for the DDM as the structure could be designed in a lighter and integrated way.The reliability of the serviceability limit state for HSS moment frames considering roof drift was therefore investigated in this study. The wind load for considering serviceability is taken as the peak wind

410 load in a 10-yearreference period (W_{10yr}). Studies have found that a Type 1 Extreme Value
411 distribution can model W_{10yr}, with a mean = $0.65W_n$ and a COV = 0.5 [33, 35]. It is shown that
412 the 10-yr wind load can be obtained by multiplying the 50-yr wind load by a conversion factor
413 of 0.7 [35]. Therefore, a load of $0.7W_n$ was used to check wind drift serviceability. Note that the
414 serviceability check does not involve using the resistance factors. The criterion for roof wind is
415 assumed to be H/300, with H representing the building height. The probabilities of exceeding
416 the wind drift are summarised in Table 7 for the sample baseline frames and wind load cases.
417 Note that these failure probabilities are for a ten-year reference period. The last column of Table
418 7 gives the corresponding annual reliability indices for the roof drift limit state. The annual
419 serviceability reliability indices vary between 1.6 and 2.1. The corresponding annual probability
420 of exceedance is approximately from 0.018 to 0.05. The reliability of wind drift appears to be
421 adequate, as the Serviceability Appendix in ASCE 7 suggests an annual serviceability limit state
422 probability on the order of 0.05 to 0.1 [13].
423

424 ## 6. Conclusion

425 To develop the Direct Design Method, sixteen 3D cold-formed HSS frames were analysedfor
426 their system reliabilities using advanced finite element analysis and Monte Carlo simulations.
427 The system resistance factors (ϕ_s) were established for the sixteen baseline frames for different
428 levels of target reliability index (β). The system reliability analysis results show that although
429 the frames have different layout, geometries and failure modes, the probabilistic characteristics
430 of the frames' ultimate strength are comparable, suggesting similar values of ϕ_s for all the HSS
431 frames considered in this study.
432
433 If the target system reliability index for the cold-formed HSS frames designed by the DDM under
434 gravity loads is assumed to fall in the range 2.5 to 2.75, the system resistance factor would be
435 ranged between 0.85–0.90 to achieve this target. This range of system resistance factor would
436 lead to a reliability index between 2.25 to 2.5 for the combined gravity and wind loads.
437
438 Moreover, the serviceability reliability for HSS moment frames subjected to service wind load
439 was investigated. It was found that the annual drift reliability indices vary from 1.6 to 2.1under
440 a 10-year service wind load.
441

442 ## References

443

1. N. S. Trahair, S.L., Chan, *Out-of-plane advanced analysis of steel structures.* Engineering Structures, 2003. **25**(13): p. 1627-1637.
2. R.D. Ziemian, *Advanced methods of inelastic analysis in the limit states design of steel structures.* PhD thesis, Cornell University, 1990.
3. D. W. White, J.F., Hajjar, *Stability of steel frames: the cases for simple elastic and rigorous inelastic analysis/design procedures.* Engineering Structures, 2000. **22**: p. 155-167.
4. P. Avery, M., Mahendran, *Distributed plasticity analysis of steel frame structures comprising non-compact sections.* Engineering Structures, 2000. **22**: p. 901-919.
5. S.E. Kim, M.H., Park., S.H, Choi, *Direct design of three-dimensional frames using practical advanced analysis.* Engineering Structures, 2001. **23**: p. 1491-1502.
6. H.V. Long, N.D., Hung, *Local buckling check according to eurocode-3 for plastichinge analysis of 3-d steel frames.* Engineering Structures, 2008. **30**: p. 3105-3113.
7. X.Z. Zhao, L.S., Dai, T. Wang, Y.Y. Chen, *A theoretical model for the rotational stiffness of storage rack beam-to-upright connections.* Journal of Constructional Steel Research, 2017. **133**: p. 269-281.
8. AS4100, *Steel structures.* Standards Australia, Sydney, Australia, 1998.
9. AISC360-10, *Specification for structural steel buildings.* American Institute of Steel Construction (AISC), Chicago,Illinois, 2010.
10. *System reliabilities of steel frames designed by the inelastic analysis and design method in AISC 360-10.* Journal of Structural Engineering, ASCE, Submitted to (H.Zhang, H.Liu, B.R. Ellingwood, K.J.R. Rasmussen).
11. AISC-LRFD, *Manual of steel construction, load and resistance factor design.* American Institute of Steel Construction (AISC), 2010.
12. B. R. Ellingwood, *LRFD: implementing structural reliability in professional practice.* Engineering Structures, 2000. **22**: p. 106-115.
13. ASCE7-05, *Minimum design loads for buildings and other structures.* ASCE,Reston,VA., 2006.
14. R.D. Ziemian, W., McGuire, G.G, Dierlein *Inelastic limit states design. Part I: planar frame studies.* Journal of Structural Engineering, ASCE, 1992. **118**(9): p. 2532-2549.
15. Q. Li, B.R., Ellingwood, *Damage inspection and vulnerability analysis of existing buildings with steel moment-resisting frame.* Engineering Structures, 2008. **30**: p. 338-351.
16. H. Dai, H., Zhang, *A Multiwavelet Netural Network-Based Response Surface Method for Structural Reliability Analysis.* Computer aided Civil and Infrastructure Engineering, 2015 **30**: p. 151-162.
17. H. Dai, G., Xue, W. Wang, *An Adaptive Wavelet Frame Neural Network Method for Efficient Reliability Analysis.* Computer aided Civil and Infrastructure Engineering, 2014. **29**(10): p. 801-814.
18. H. Dai, H., Zhang, *A wavelet support vector machine-based neural network metamodel for structural reliability assessment.* Computer aided Civil and Infrastructure Engineering, 2017. **32**: p. 344-357.
19. R.E. Melchers, *Structural reliability analysis and prediction.* John Wiley & Sons, 1999.
20. H. Zhang, T., Chandrangsu, K.J.R, Rasmussen, *Probabilistic study of the strength of steel scaffold systems.* Structrural Safety, 2010(32): p. 393-401.
21. B.R. Ellingwood, T.V.G., *Probability-based criteria for structural design.* Structural Safety, 1982. **1**: p. 15-26.
22. H. Zhang, S., Shayan, K. J. R. Rasmussen, B. R. Ellingwood, *System-based design of planar steel frames, II: reliability results and design recommendations.* Journal of Constructional Steel Research, 2016. **123**: p. 154-161.

23. H. Zhang, S., Shayan, K. J. R, Rasmussen, B. R, Ellingwood, *System-based design of planar steel frames, I: reliability framework.* Journal of Constructional Steel Research, 2016. **123**: p. 135-143.
24. K. J. R. Rasmussen, G.J., Hancock, *Geometric imperfections in plated structures subject to interaction between buckling modes.* Thin-Walled Structures, 1988. **6**(6): p. 433-452.
25. S. Shayan, K.J.R., Rasmussen, H. Zhang *On the modelling of initial geometric imperfections of steel frames in advanced analysis.* Journal of Constructional Steel Research, 2014. **98**: p. 167-177.
26. C.E.A.C.M, *Laboratory report, commission 8.* Politecnico di Milano, Istituto,di Scienza delle Construzioni, Laboratorio Prove Materiali, 1966.
27. T. Wilkinson, G.J., Hancock, *Tests for the compact web slenderness of cold-formed rectangular hollow sections.* Research Report R744, Centre for Advanced Structural Engineering, Department of Civil Engineering, The University of Sydney, 1997.
28. W. Liu, *Sytem Reliability-Based Design of Three-Dimensional Steel Structures by Advanced Analysis.* PhD thesis, The University of Sydney, 2016.
29. W. Liu., K.J.R., Rasmussen., H, Zhang, *Modelling and probabilistic study of the residual stress of cold-formed hollow steel sections.* Engineering Structures, 2017. **150**: p. 986-995.
30. X. Zhang, K.J.R., Rassmussen, H. Zhang, *Experimental investigation of locally and distortionally buckled portal frames.* Journal of Constructional Steel Research, 2016. **122**: p. 571-583.
31. A. N. Trouncer, K.J.R., Rasmmusen, *Ultra-light gauge steel storage rack frames. Part 1: Experimental investigations.* Journal of Constructional Steel Research, 2016. **124**: p. 57-76.
32. W. Liu, K.J.R., Rasmussen, H. Zhang, *Systems Reliability for 3D Steel Frames Subject to Gravity Loads.* Structures, 2016. **8, Part 2**: p. 170-182.
33. B.R. Ellingwood, T.V., Galambos, J.G.MacGregor and C.A.Cornell, *Development of a probability based load criterion for american national standard A58: Building code requirements for minimum design loads in buildings and other structures.* U.S. Department of Commerce, National Bureau of Standards, 1980.
34. Ellingwood, B.R., *Probability-based codified design: past accomplishments and future challenges.* Structrural Safety, 1994. **13**: p. 159-176.
35. D. Rosowsky, *Estimation of design loads for reduced reference periods.* Structural Safety, 1995. **17**: p. 17-32.

531 Table 1: Statistics of the basic random variables.

	Mean	COV	Distribution	Reference
E	E_n	0.06	Normal	[37]
F_y	$1.1F_{yn}$	0.1	Lognormal	[37]
t	$0.964t_n$	0.039	Normal	[38]
D	$1.05D_n$	0.10	Normal	[21]
L	L_n	0.25	Extreme Type 1	[21]
L_{apt}	$0.25L_n$	0.60	Gamma	[21]
W	$0.96W_n$	0.37	Extreme Type 1	[21]

COV= coefficient of variation

532
533

534 Table 2: Statistical data of geometric imperfection scale factors for HSS.

	a_1	a_2	a_3
μ	$1.26\times10^{-4}L$	$4.08\times10^{-5}\,L$	$2.2\times10^{-5}\,L$
σ	$1.62\times10^{-4}\,L$	$5.16\times10^{-5}\,L$	$2.81\times10^{-5}\,L$

535

536

537 Table 3: System resistance factors (ϕ_s) for HSS moment frames under gravity loads.

Sway Frame	Failure Mode	Mean/nominal	COV	ϕ_s			
				β=2.50	β=2.75	β=3.0	β=3.50
Frame 1	BFY-CFY	1.06	0.119	0.88	0.83	0.78	0.68
	BFY-CPY	1.06	0.110	0.86	0.81	0.77	0.67
	BFY	1.08	0.123	0.89	0.84	0.79	0.69
	SWAY-CPY	0.99	0.099	0.84	0.80	0.75	0.66
Frame 2	BFY-CFY	1.04	0.114	0.85	0.80	0.75	0.65
	BFY-CPY	1.03	0.121	0.83	0.78	0.73	0.64
	BFY	1.05	0.106	0.86	0.81	0.76	0.67
	SWAY-CPY	1.01	0.091	0.87	0.82	0.77	0.68
Frame 3	BFY-CFY	1.05	0.111	0.88	0.83	0.78	0.68
	BFY-CPY	1.06	0.106	0.87	0.82	0.77	0.68
	BFY	1.05	0.111	0.86	0.81	0.76	0.67
	SWAY-CPY	1.02	0.090	0.88	0.83	0.78	0.68
Frame 4	BFY-CFY	1.04	0.109	0.87	0.82	0.77	0.67
	BFY-CPY	1.02	0.106	0.86	0.81	0.76	0.66
	BFY	1.06	0.119	0.88	0.84	0.79	0.69
	SWAY-CPY	1.01	0.090	0.87	0.82	0.78	0.68
Frame 5	BFY-CFY	1.03	0.098	0.86	0.81	0.76	0.67
	BFY-CPY	1.04	0.097	0.89	0.84	0.79	0.69
	BFY	1.04	0.111	0.86	0.81	0.77	0.67
	SWAY-CPY	1.05	0.097	0.90	0.85	0.80	0.70
Frame 6	BFY-CFY	1.04	0.109	0.84	0.79	0.75	0.65
	BFY-CPY	1.04	0.102	0.88	0.83	0.78	0.68
	BFY	1.05	0.115	0.86	0.81	0.76	0.67
	SWAY-CPY	1.03	0.098	0.88	0.83	0.79	0.69
Frame 7	BFY-CFY	1.05	0.110	0.88	0.83	0.78	0.68
	BFY-CPY	1.08	0.117	0.88	0.83	0.78	0.68
	BFY	1.05	0.118	0.87	0.82	0.78	0.68
Frame 8	BFY	1.05	0.096	0.90	0.85	0.80	0.70
	BPY-CPY	1.01	0.094	0.87	0.82	0.77	0.68
	SWAY-CPY	0.99	0.094	0.85	0.80	0.75	0.66
Average ϕ_s				0.87	0.82	0.77	0.67

538

539

Table 4: Weights for gravity loads $D + L$ for cold-formed steel structures [34].

L_n/D_n	1.0	1.5	2.0	3.0	5.0
Weight (%)	6%	17%	22%	33%	22%

Table 5: System resistance factors (ϕ_s) for HSS moment frames subjected to combined gravity and wind loads.

Sway Frame	Failure Mode	ϕ_s			
		β=2.25	β=2.5	β=2.75	β=3
Frame 1 (Wind Load Case 3)	CFY	0.91	0.82	0.73	0.66
Frame 2 (Wind Load Case 3)	BFY-CFY	0.90	0.81	0.74	0.67
Frame 3 (Wind Load Case 1)	BFY-CFY	0.92	0.83	0.75	0.67
Frame 4 (Wind Load Case 1)	BFY-CFY	0.88	0.80	0.72	0.65
Frame 5 (Wind Load Case 1)	BFY-CFY	0.92	0.82	0.74	0.66
Frame 6 (Wind Load Case 1)	BFY-CFY	0.92	0.82	0.74	0.66
Frame 7 (Wind Load Case 1)	BFY-CFY	0.90	0.81	0.73	0.65
Frame 8 (Wind Load Case 1)	BFY-CFY	0.86	0.78	0.71	0.64
Average ϕ_s		0.90	0.81	0.73	0.66

549 Table 6: System resistance factors (ϕ_s) for HSS braced frame subject to gravity loads.

Braced Frame	Failure Mode	Mean/nominal	COV	ϕ_s			
				β=2.50	β=2.75	β=3.0	β=3.5
Frame 1	CPY	0.97	0.080	0.84	0.80	0.75	0.66
Frame 2	BFY	0.97	0.077	0.83	0.79	0.74	0.65
	CPY	0.99	0.071	0.87	0.82	0.78	0.68
Frame 3	BFY	1.06	0.118	0.88	0.83	0.78	0.68
	CPY	1.04	0.079	0.91	0.86	0.81	0.71
Frame 4	BFY	1.07	0.111	0.90	0.85	0.80	0.70
	CPY	1.00	0.084	0.85	0.81	0.76	0.67
Frame 5	BFY	1.07	0.124	0.88	0.83	0.78	0.68
	BPY-CPY	0.98	0.084	0.85	0.80	0.76	0.66
Frame 6	BFY	1.06	0.117	0.89	0.84	0.79	0.69
	CPY	0.97	0.085	0.84	0.79	0.75	0.66
Frame 7	BFY	1.08	0.122	0.89	0.84	0.79	0.69
	CPY	1.03	0.099	0.88	0.83	0.78	0.68
Frame 8	BFY	1.02	0.095	0.88	0.83	0.78	0.69
	BFY-CPY	1.00	0.091	0.86	0.81	0.77	0.67
Average ϕ_s				0.87	0.82	0.78	0.68

550

551

552 Table 7: Nominal roof drift ratios and annual reliability indices (roof drift limit state) for
553 selected HSS moment frames.

	Nominal roof drift ratios	$P_{f(10yr)}$	$\beta_{(1yr)}$
Frame 1 (Wind Load Case 1)	*H*/313	0.362	1.706
	H/354	0.263	1.879
	H/397	0.194	2.027
Frame 1 (Wind Load Case 3)	*H*/309	0.392	1.660
	H/345	0.307	1.800
	H/396	0.197	2.019
Frame 2 (Wind Load Case 1)	*H*/300	0.403	1.642
	H/333	0.329	1.762
	H/428	0.164	2.103
Frame 2 (Wind Load Case 3)	*H*/300	0.421	1.614
	H/372	0.264	1.879
	H/408	0.213	1.984
Frame 3 (Wind Load Case 1)	*H*/313	0.361	1.708
	H/347	0.267	1.872
	H/427	0.151	2.139
Frame 5 (Wind Load Case 1)	*H*/316	0.372	1.691
	H/375	0.260	1.885
	H/435	0.156	2.124

554
555
556
557

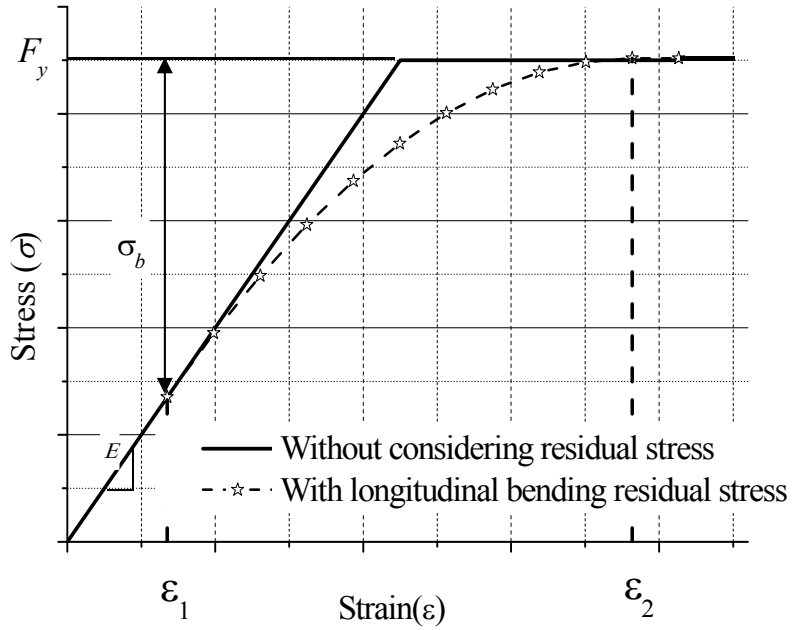

558

559 Fig.1: Stress-strain curves with and without considering longitudinal bending residual stress.

560

561

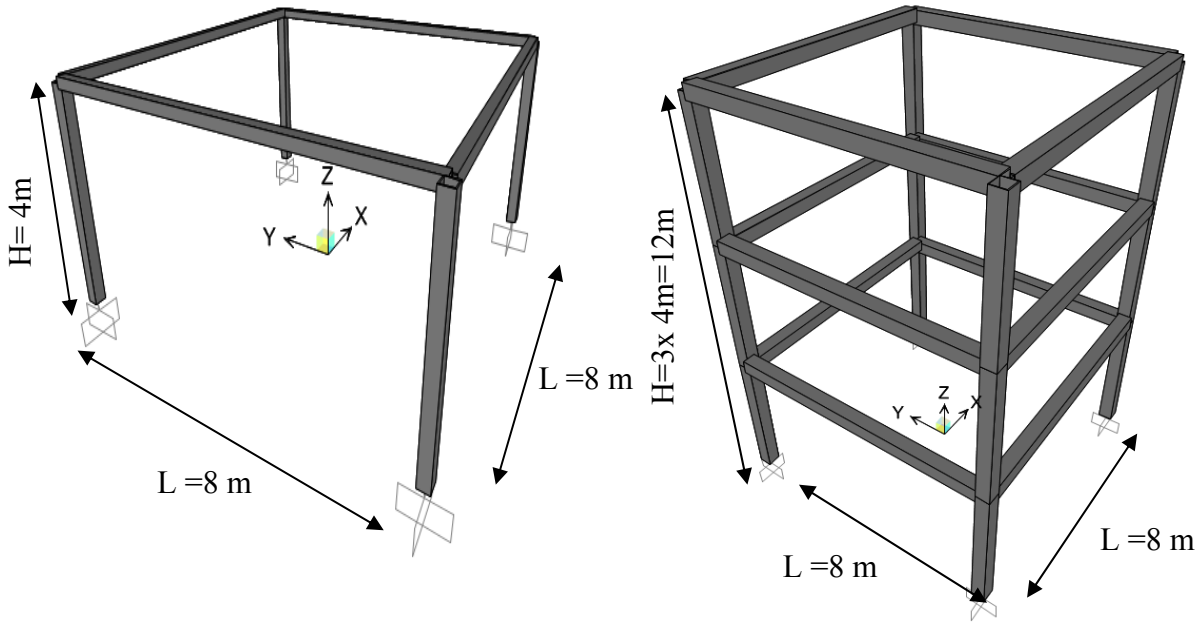

Moment Frame 1 Moment Frame 2

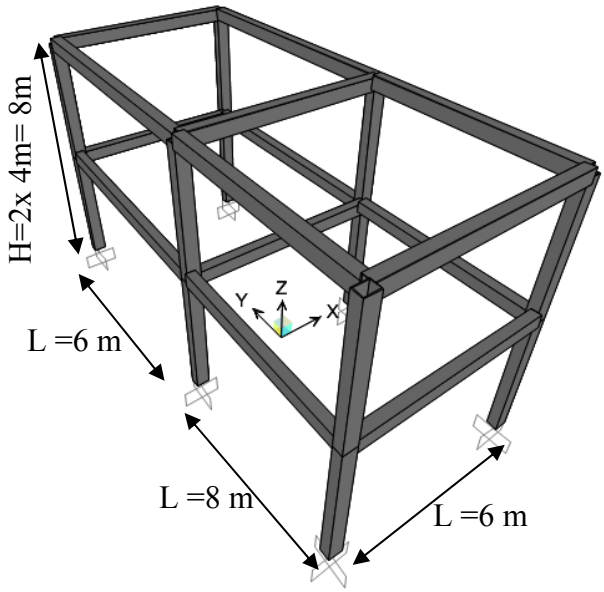

Moment Frame 3

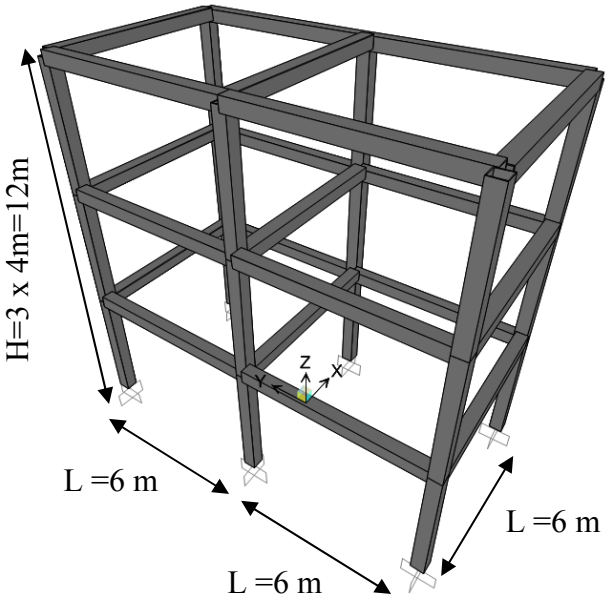

Moment Frame 4

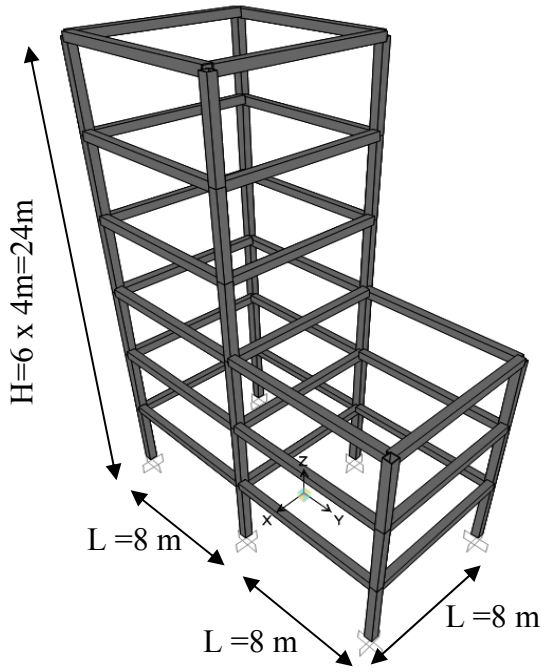

Moment Frame 5

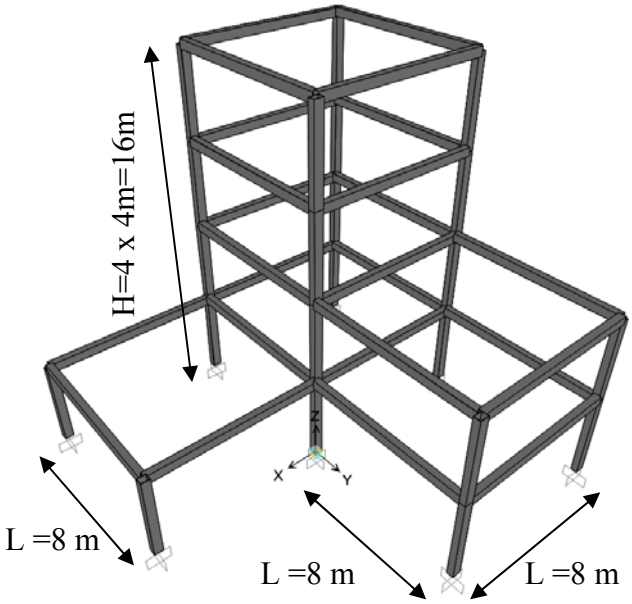

Moment Frame 6

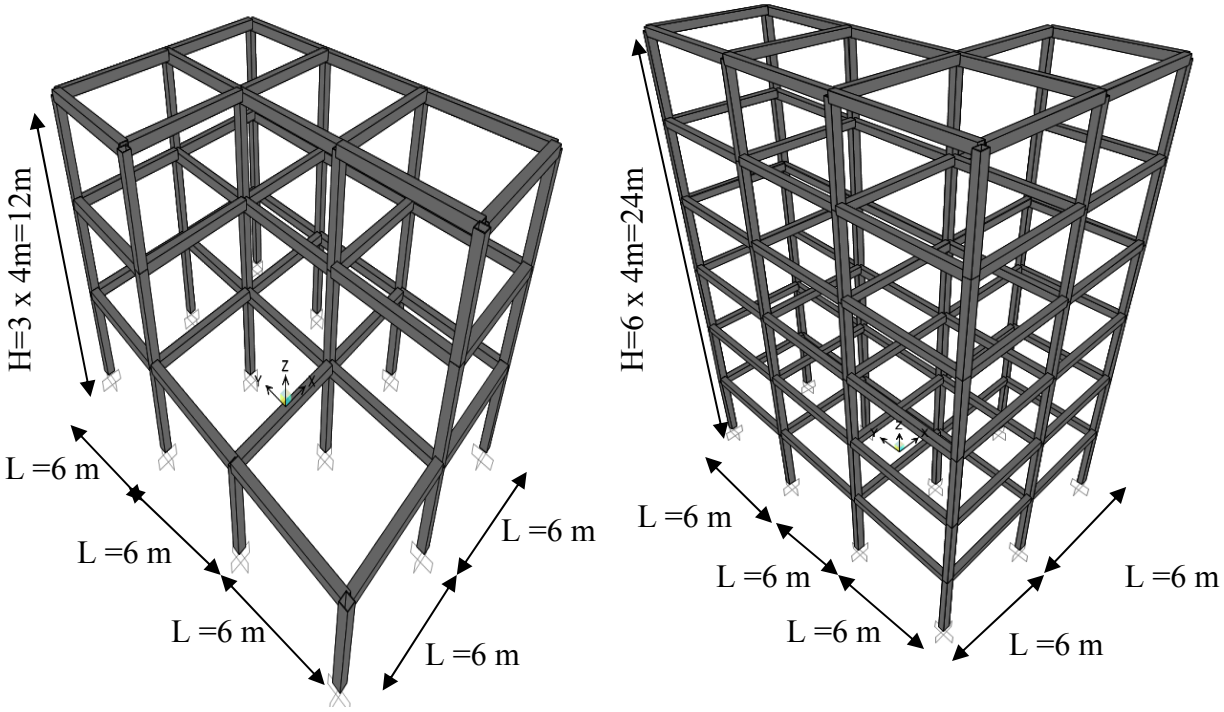

Moment Frame 7 Moment Frame 8

562
563 Fig.2: Layouts for 3D HSS moment frame systems.
564
565

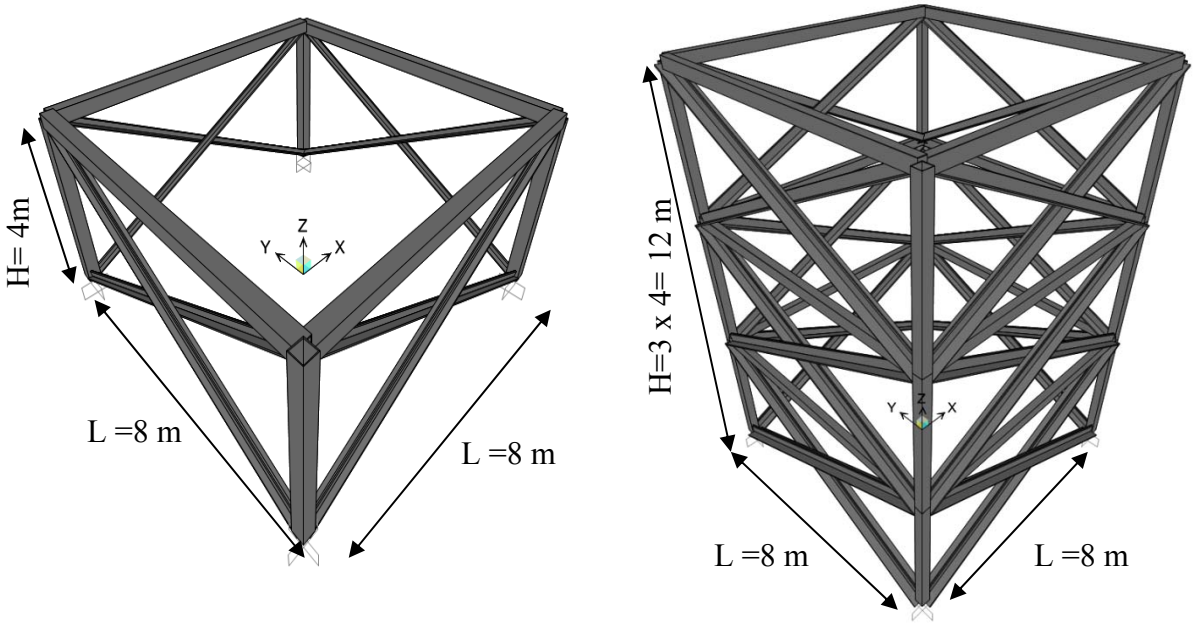

Braced Frame 1 Braced Frame 2

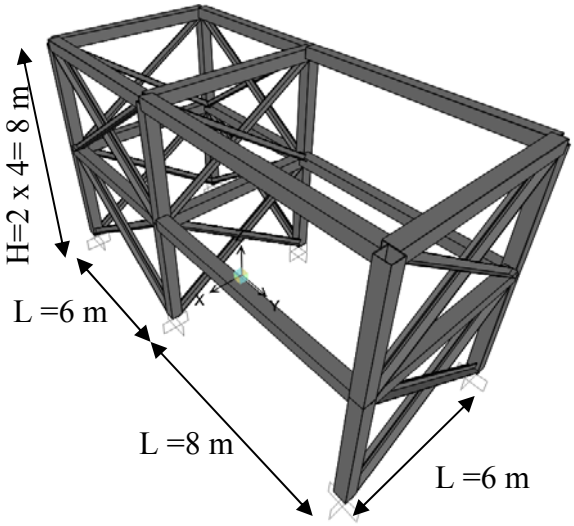

Braced Frame 3

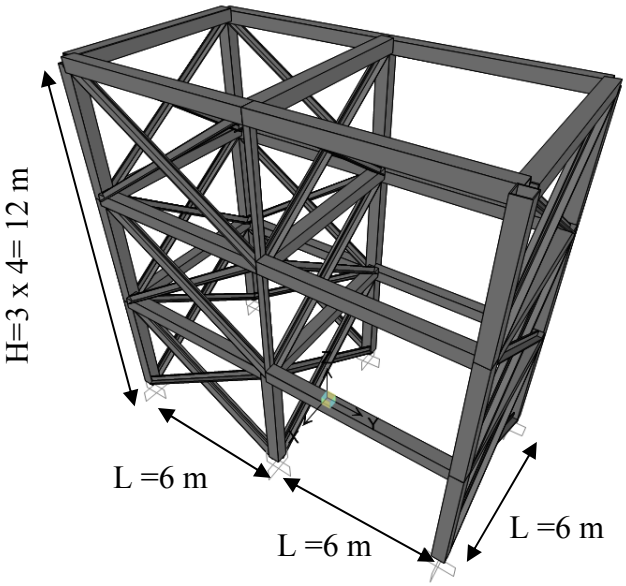

Braced Frame 4

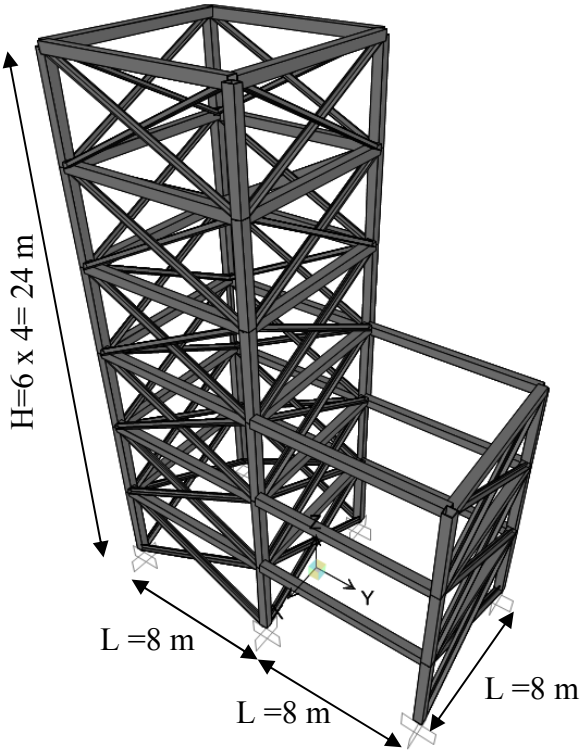

Braced Frame 5

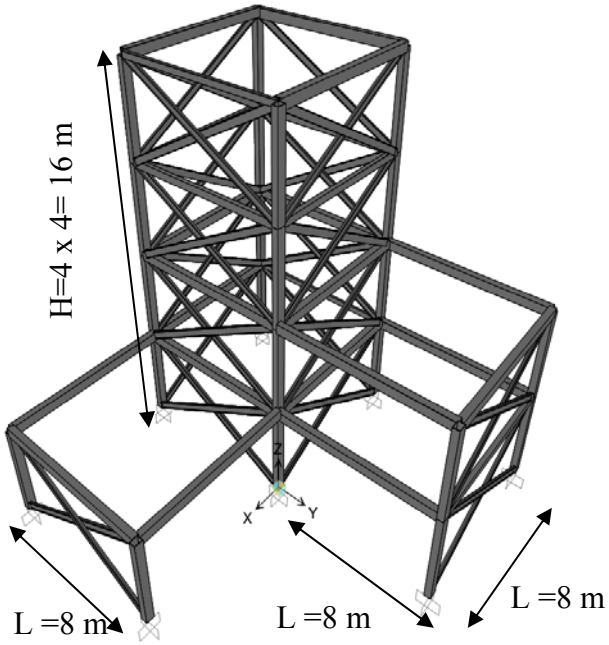

Braced Frame 6

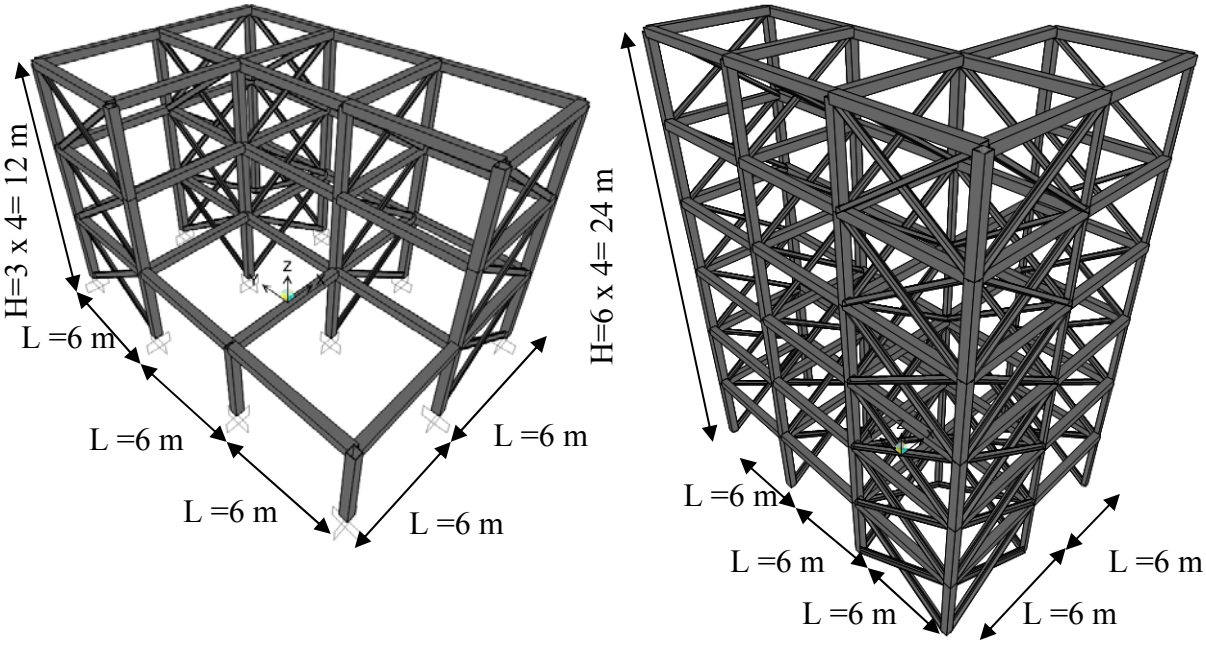

Braced Frame 7 Braced Frame 8

Fig.3: Layouts for 3D HSS braced frame systems.

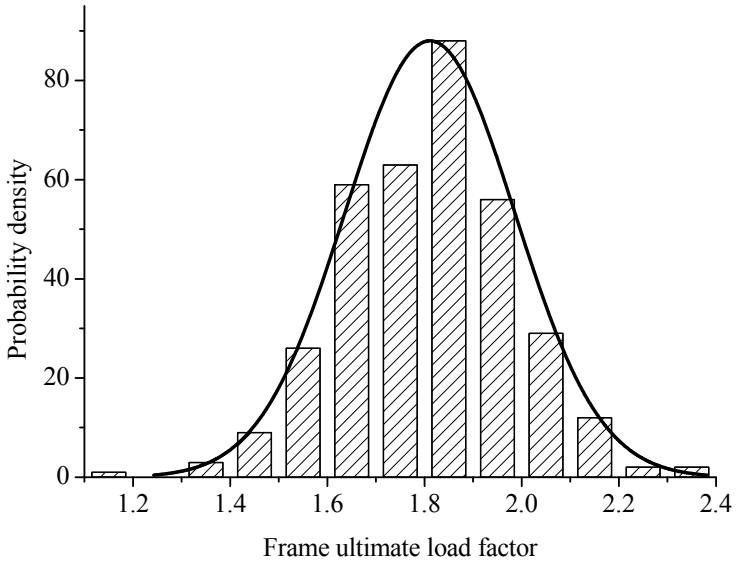

(a) Histogram of ultimate gravity strength factor for moment Frame 3 with a failure mode of BFY-CFY.

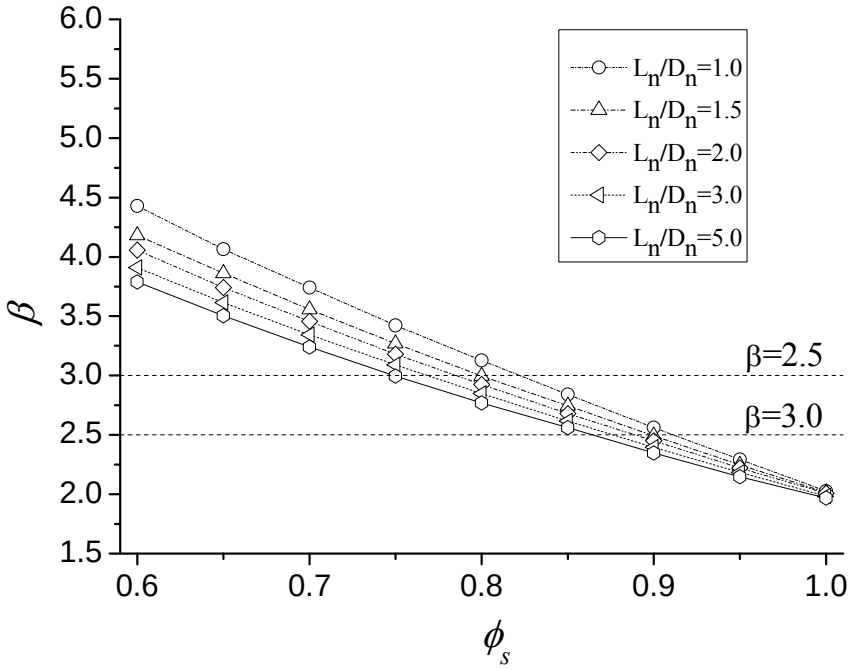

(b) β-ϕ_s curve

Fig. 4: Moment Frame 3 under gravity loads, failure mode BFY-CFY.

571

572

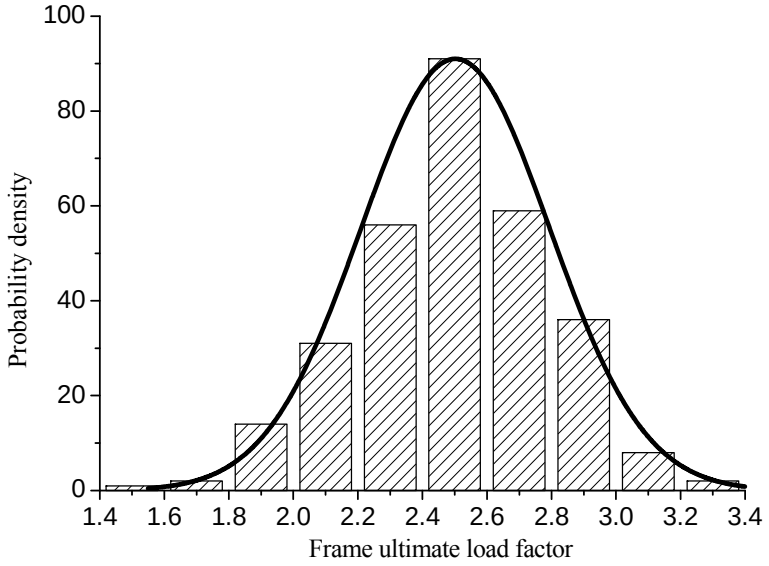

Fig. 5: Histogram of the ultimate lateral strength factor for moment Frame 3.

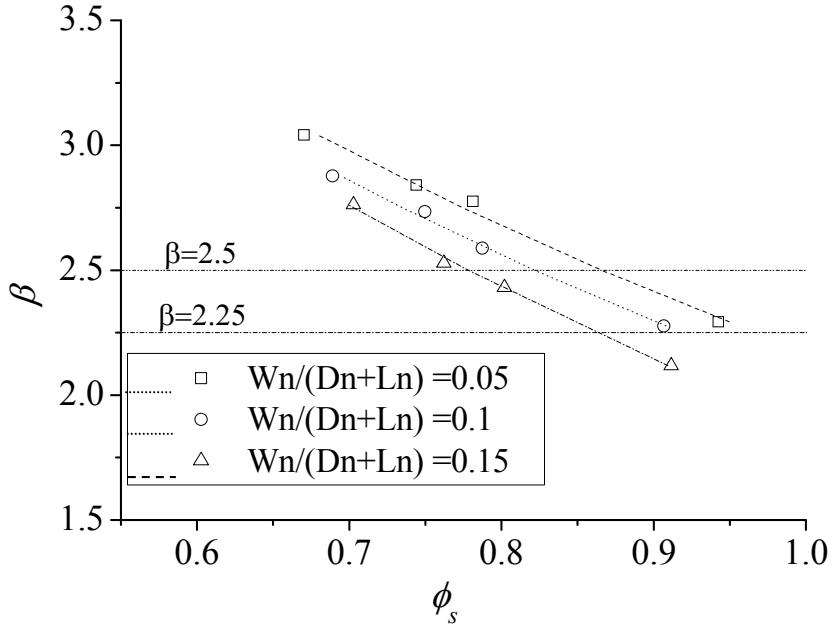

Fig. 6: β-ϕ_s curve for moment Frame 3 under combined gravity and wind loads, failure mode: BFY-CFY.

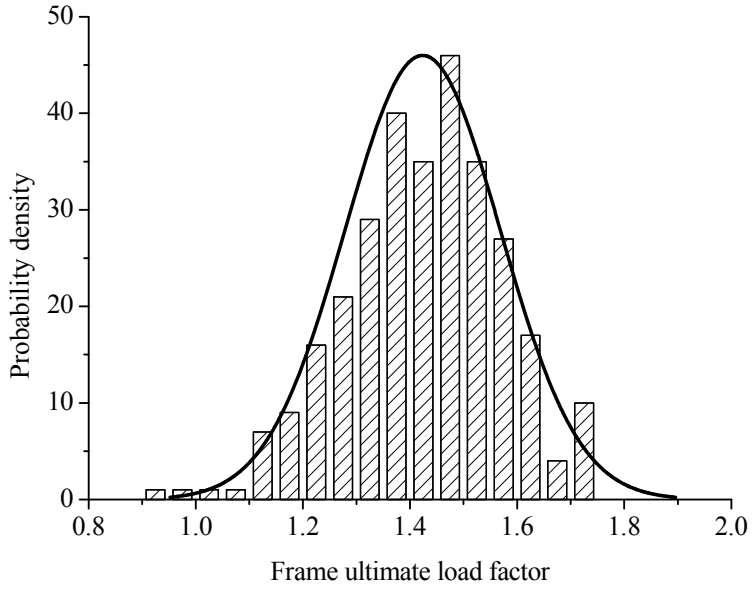

(a) Histogram of ultimate gravity strength factor for HSS Braced Frame 3 with a failure mode of BFY.

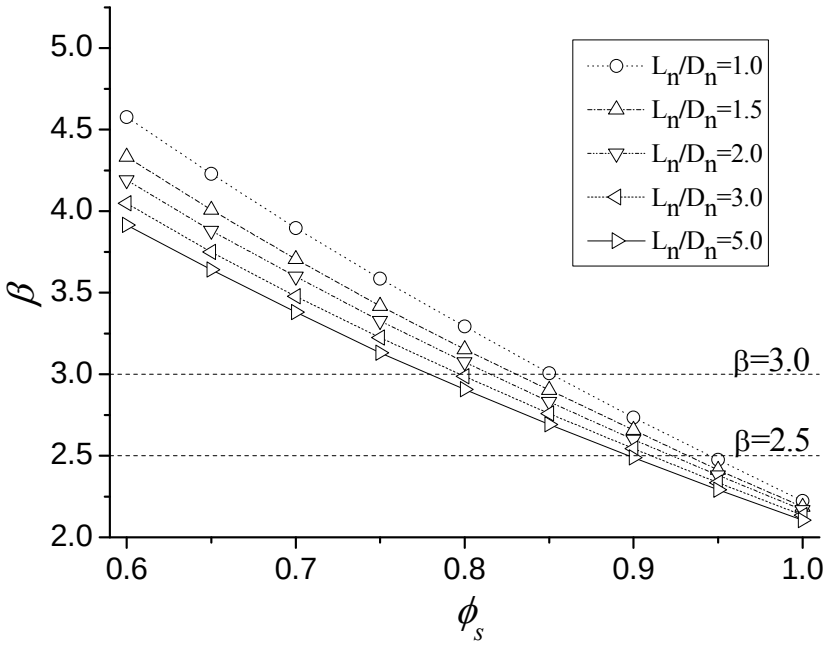

(b) β-ϕ_s curve for HSS Braced Frame 3

Fig. 7: Braced Frame 3 subjected to gravity load only, failure mode: BFY

573
574